CFD Project 3 - Numerical Simulation of Isoentropic Flow Through a CD Nozzle

Aditya Prasad (22110018)

Department of Mechanical Engineering, IIT Gandhinagar

Instructor: Prof. Dilip S. Sundaram

Contents

1. Introduction

CD nozzles play a vital role in various applications, especially in aerospace, where they are instrumental in accelerating combustion gases to generate thrust in rockets. In this project, we assume quasi-one-dimensional, inviscid, unsteady, compressible flow with adiabatic conditions along the nozzle walls. Using the finite difference method (FDM) and MacCormack's scheme for discretization, we aim to solve the time-dependent Euler equations to achieve a steady-state solution across different flow regimes. Specifically, the project will explore purely subsonic flow and subsonic-to-supersonic flows.

2. Governing Equations

To simulate the flows, we will try to solve the Euler equations which are just the differential forms of the conservation of mass, momentum and energy. Euler equations are tailor made for Quasi-1dimensional, inviscid, and compressible CD nozzle flows.

2.1. Non-Dimensionlising Primitive variables:

We can define non-dimensional density with respect to the Stagnation density as

$$\rho' = \frac{\rho}{\rho_0} \tag{1}$$

where (for the time being) the prime denotes a dimensionless variable.

We define dimensionless length as

$$x' = \frac{x}{L} \tag{2}$$

Denoting the speed of sound in the reservoir as a_0, where

$$a_0 = \sqrt{\gamma R T_0}$$

We define a dimensionless velocity as

$$V' = \frac{V}{a_0} \tag{3}$$

Also, the quantity L/a_0 has the dimension of time, and we define a dimensionless time as

$$t' = \frac{t}{L/a_0} \tag{4}$$

Finally, we take the ratio local area A to the sonic throat area A^* and define a dimensionless area as

$$A' = \frac{A}{A^*} \tag{5}$$

We can non-dimensionalize Pressure P with respect to the stagnation pressure P_0 as

$$P' = \frac{P}{P_0}$$

From the Ideal Gas State equation we have

$$P' \cdot P_0 = \rho' \cdot \rho_0 \cdot R \cdot T' \cdot T_0$$

$$\Rightarrow P' = \rho' \cdot T' \tag{6}$$

We can non-dimensionalize internal energy e with respect to the stagnation temperature.

We can define nondimensional internal energy as follows:

$$e' = \frac{e}{e_0} \tag{7}$$

where $e_0 = c_v T_0 = \frac{RT_0}{\gamma - 1}$

We define nondimenstional temperature with respect to the stagnation temperature as follows:

$$T' = \frac{T}{T_0}$$

Since $e_0 = c_v T_0 = \frac{RT_0}{\gamma - 1}$

We can equate non-dimensionalized temperature with non-dimensionalized internal energy as

$$T' = e' \tag{8}$$

2.2. Non-Dimenstionlising Conservation Equations

Non-dimenstionalized Continuity Equation

$$\frac{\partial(\rho A)}{\partial t} + \frac{\partial(\rho A V)}{\partial x} = 0 \tag{9}$$

This is the continuity equation for quasi-one-dimensional flow. It is already in conservation form. Nondimensionalizing the variables according to the forms given in the section above, we have

$$\frac{\partial}{\partial t}\left(\frac{\rho A}{\rho_0 A^*}\right) + \frac{\partial}{\partial (x/L)}\left(\frac{\rho' A' V'}{\rho_0 A^* a_0}\right) = 0 \tag{10}$$

or

$$\frac{\partial(\rho' A')}{\partial t'} + \frac{\partial(\rho' A' V')}{\partial x'} = 0 \tag{11}$$

Non-dimensionalized X-momentum Equation:

$$\frac{\partial(\rho A V)}{\partial t} + \frac{\partial(\rho A V^2)}{\partial x} = -A\frac{\partial p}{\partial x} \tag{12}$$

This is the momentum equation for quasi-one-dimensional flow. It is already in conservation form. Let us combine the two x derivatives as follows.

Using the product rule, we have

$$\frac{\partial(\rho A)}{\partial x} = \rho\frac{\partial A}{\partial x} + A\frac{\partial \rho}{\partial x} \tag{13}$$

Upon substituting the last term, we have

$$\frac{\partial(\rho A V)}{\partial t} + \frac{\partial(\rho A V^2 + pA)}{\partial x} = \rho V\frac{\partial A}{\partial x} \tag{14}$$

Nondimensionalizing the above equation, we have

$$LHS = \frac{\partial}{\partial t}\left(\frac{\rho A V}{\rho_0 A^* a_0}\right) + \frac{\partial}{\partial (x/L)}\left[\frac{\rho A V^2}{\rho_0 A^* a_0^2} + \frac{pA}{\rho_0 A^* a_0^2} + \frac{A}{\rho_0 A^*}(\rho A^2)\right]$$

$$RHS = \frac{\rho}{\rho_0}\frac{\partial(A/A^*)}{\partial(x/L)}\left(\frac{\rho_0 A^*}{L}\right)$$

Hence we can substitute by the dimensionalized terms,

$$\frac{\partial(\rho' A' V')}{\partial t'} + \frac{\partial(\rho' A' V'^2 + p' A'/(\rho_0 a_0^2))}{\partial x'} = p'\frac{\partial A'}{\partial x'}\left(\frac{\rho_0}{p_0 a_0^2}\right) \tag{15}$$

However, using the state equation,

$$\frac{p_0}{\rho_0 a_0^2} = \frac{\rho_0 R T_0}{\rho_0^2 a_0^2} = \frac{\rho_0 R T_0}{\rho_0^2(\gamma R T_0)} = \frac{1}{\gamma} \tag{16}$$

Thus, we have the final equation as,

$$\frac{\partial(\rho' A' V')}{\partial t'} + \frac{\partial(\rho' A' V'^2 + (1/\gamma)p' A')}{\partial x'} = \frac{1}{\gamma}p'\frac{\partial A'}{\partial x'} \tag{17}$$

Non-dimensionalized Energy equation:

$$\frac{\partial[\rho(e + \frac{V^2}{2})A]}{\partial t} + \frac{\partial[\rho(e + \frac{V^2}{2})AV]}{\partial x} = -\frac{\partial(pAV)}{\partial x} \tag{18}$$

This is the energy equation for quasi-one-dimensional flow. It is already in conservation form. Combining the x derivatives in the above equation, we have

$$\frac{\partial[\rho(e + \frac{V^2}{2})A]}{\partial t} + \frac{\partial[\rho(e + \frac{V^2}{2})AV + pAV]}{\partial x} = 0 \tag{19}$$

Upon introducing reference values into the above equation,

$$LHS = \frac{\partial}{\partial t}\left[\frac{\rho}{p_0}\left(\frac{e}{e_0} + \frac{V^2}{2a_0^2}\right)A^*\right]$$

$$RHS = \frac{\partial}{\partial(x/L)}\left[\frac{\rho A' V'}{p_0 A^* a_0}\left\{\frac{p}{p_0}\left(\frac{e}{e_0} + \frac{V^2}{2a_0^2}\right)A^* + \frac{pA'V'}{p_0 A^* a_0}\right\}\right] = 0$$

Divide by $\rho_0 A^* a_0 R T_0/L$ on both sides,

$$LHS = \frac{\partial}{\partial t'}\left[\rho'\left(\frac{e'}{\gamma - 1} + \frac{V'^2}{2}\right)A'\right]$$

$$RHS = \frac{\partial}{\partial x'}\left[\rho'\left(\frac{e'}{\gamma - 1} + \frac{V'^2}{2}\right)V'A' + p'A'V'\left(\frac{p_0}{\rho_0 R T_0}\right)\right]$$

However, in the above equation,

$$\frac{p_0}{\rho_0 R T_0} = \frac{\rho_0 R T_0}{\rho_0^2 R T_0} = 1$$

Thus, we have the final non-dimensionalized energy conservation equation as,

$$\frac{\partial}{\partial t'}\left[\rho'\left(\frac{e'}{\gamma - 1} + \frac{V'^2}{2}\right)A'\right] + \frac{\partial}{\partial x'}\left[\rho'\left(\frac{e'}{\gamma - 1} + \frac{V'^2}{2}\right)V'A' + p'A'V'\right] = 0 \tag{20}$$

2.3. Conservation Equations in generic form:

Equations (11), (17), and (20) are the nondimensional conservation form of the continuity, momentum, and energy equations for quasi-one-dimensional flow, respectively. We define a generic form of the governing equations for unsteady, three-dimensional flow. Let us define the elements of the solutions vector U, the flux vector F, and the source term J as follows.

$$\begin{aligned}
U_1 &= \rho' A' \\
U_2 &= \rho' A' V' \\
U_3 &= \rho'\left(\frac{e'}{\gamma - 1} + \frac{V'^2}{2}\right)A' \\
F_1 &= \rho' A' V' \\
F_2 &= \rho' A' V'^2 + p' A' \\
F_3 &= \rho'\left(\frac{e'}{\gamma - 1} + \frac{V'^2}{2}\right)V'A' + p'A'V' \\
J_1 &= 0 \\
J_2 &= \frac{1}{\gamma}p'\frac{\partial A'}{\partial x'}
\end{aligned}$$

With these elements, Eqs. (11), (17), and (20) can be written, respectively, as

$$\frac{\partial U_1}{\partial t'} = -\frac{\partial F_1}{\partial x'} \tag{21}$$

$$\frac{\partial U_2}{\partial t'} = -\frac{\partial F_2}{\partial x'} + J_2 \tag{22}$$

$$\frac{\partial U_3}{\partial t'} = -\frac{\partial F_3}{\partial x'} \tag{23}$$

These are the mass, energy, and momentum conservation equations in conservative forms, which we wish to solve using MacCormack's scheme. We wish to solve for conserved variables Q_1, Q_2, Q_3 after which we can extract the primitive variables p', ρ', T', u'. The solution vector for our numerical scheme is the vector of Q's as $[Q_1, Q_2, Q_3]$.

3. Grid Discretization

We divide the x-axis along the nozzle into a number of discrete grid points. The first grid point labeled 1 is said to be the reservoir having stagnation properties. The points are evenly distributed along the x-axis, with the spacing between them represented by Δx. The last grid point labelled N is the nozzle exit.

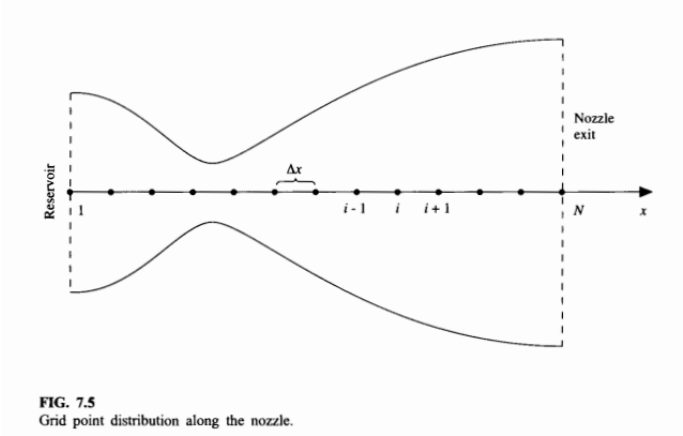

FIG. 7.5
Grid point distribution along the nozzle.

Figure 1. Grid Discretization in the nozzle

Nozzle Geometry

A symmetric converging-diverging nozzle is to be considered. The nozzle geometry is described by the area function as given below:

$$A = 1 + 2.2(x - 1.5)^2, \quad 0 \le x \le 3 \tag{24}$$

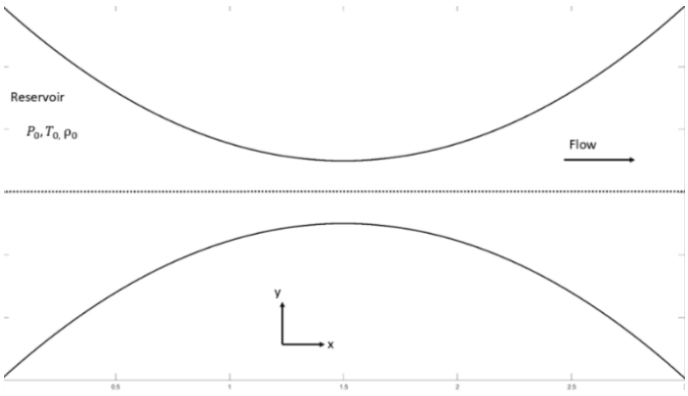

Figure 2. Nozzle geometry in the nozzle

4. Numerical Analysis of Subsonic-Supersonic Flow :

4.1. Boundary Conditions

Subsonic Inflow Boundary

The boundary conditions for the subsonic-supersonic isentropic flow solution at the subsonic inflow boundary two properties are held fixed and one is allowed to float. We hold ρ' and T' fixed at the inflow boundary, both equal to 1.0, and allow V' to float. By holding ρ' fixed, then U1 at grid point $i = 1$ is fixed, independent of time, via $U_1 = \rho' A'$. That is,

$$U1_{(i=1)} = (\rho' A')_{i=1} = A'_{i=1} = \text{fixed value} \tag{25}$$

The floating value of V' at the inflow boundary is calculated at the end of each time step by linearly extrapolating $U2$ from the known values at the internal grid points $i = 2$ and 3, that is,

$$U2_{(i=1)} = 2U2_{(i=2)} - U2_{(i=3)} \tag{26}$$

Since V' floats at the inflow boundary, so does the value of $U3$, which is given by

$$U3 = \rho' \left(\frac{e'}{\gamma - 1} + \frac{\gamma}{2} V'^2 \right) A' \tag{27}$$

Since $\rho' A' = U1$ and $e' = T'$, Eq. (27) is written as

$$U3 = U1 \left(\frac{T'}{\gamma - 1} + \frac{\gamma}{2} V'^2 \right) \tag{28}$$

The value of $U3_{(i=1)}$ is found by inserting the value of V' at $i = 1$, calculated above, as well as the fixed value $T' = 1$.

Supersonic Outflow Boundary

Here, we must allow all flow-field variables to float. We again choose to use linear extrapolation based on the flow-field values at the internal points. Specifically, we have, for the nondimensional variables,

$$V_N = 2V_{N-1} - V_{N-2} \tag{29}$$
$$\rho_N = 2\rho_{N-1} - \rho_{N-2} \tag{30}$$
$$T_N = 2T_{N-1} - T_{N-2} \tag{31}$$

The flow properties at the downstream, supersonic outflow boundary are obtained by linear extrapolation from the two adjacent internal points. If N denotes the grid point at the outflow boundary, then

$$(U_1)_N = 2(U_1)_{N-1} - (U_1)_{N-2} \tag{32}$$
$$(U_2)_N = 2(U_2)_{N-1} - (U_2)_{N-2} \tag{33}$$
$$(U_3)_N = 2(U_3)_{N-1} - (U_3)_{N-2} \tag{34}$$

The values of F_1, F_2, and F_3 at grid point $i = N$ are obtained from the values of U_1, U_2, and U_3 at point $i = N$

4.2. Initial Conditions

We need initial conditions for F_1, F_2, F_3 in order to start the time-marching MacCormack scheme. We give the initial conditions in the form of primitive variables ρ, T, and V at the $t = 0$ time.

The initial conditions for $U1$, $U2$, and $U3$ were synthesized by assuming the following variations of ρ' and T':

$$\rho' = 1.0 \tag{35}$$
$$T' = 1.0 \tag{36}$$

for $0 \le x' \le 0.5$

$$\rho' = 1.0 - 0.366(x' - 0.5) \tag{37}$$
$$T' = 1.0 - 0.167(x' - 0.5) \tag{38}$$

for $0.5 \le x' \le 1.5$

$$\rho' = 0.634 - 0.3879(x' - 1.5) \tag{39}$$
$$T' = 0.833 - 0.3507(x' - 1.5) \tag{40}$$

for $1.5 \le x' \le 3.0$

Since $U2$ is physically the local mass flow; that is, $U2 = \rho' A' V'$. Therefore, for the initial conditions only, let us assume a constant mass flow through the nozzle and calculate V' as

$$V' = \frac{U2}{\rho' A'} = \frac{0.59}{\rho' A'} \tag{41}$$

where we assume a generic mass flow rate which is sufficiently close to the steady state mass flow rate.

We can compare the above initial conditions of dimensionless ρ' and T' with the Analytical solution.

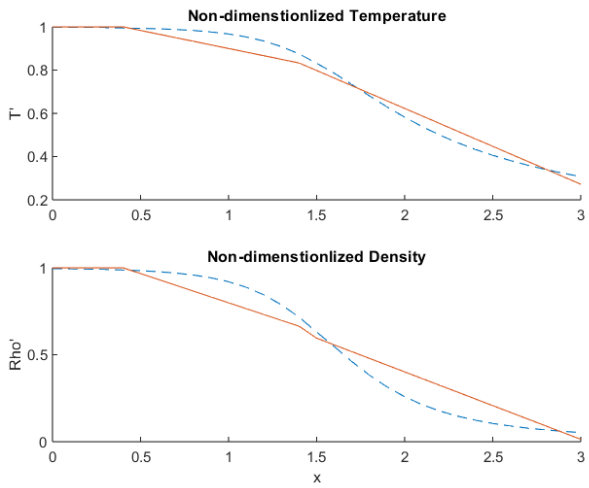

Figure 3. Comparison of Initial Conditions with Analytical Solution

4.3. Calculation of Time Step

The governing system of equations are hyperbolic with respect to time. We have the Courant Stability criteria as follows:

$$\Delta t = C\frac{\Delta x}{a+V} \tag{42}$$

Here C is the Courant number; the simple stability analysis of a linear hyperbolic equation gives the result that $C \leq 1$ for an explicit numerical solution to be stable. The present application to subsonic-supersonic flow requires a more careful consideration of the stability condition.

Here we calculate Δt at all the grid points using the values from the previous time step and take the Δt to be the minimum among those possible time step values. That is,

$$\Delta t^{n+1} = \min(\Delta t_1^n, \Delta t_2^n, ..., \Delta t_N^n) \tag{43}$$

5. Numerical Analysis of Purely Subsonic Flow :

5.1. Boundary Conditions

Subsonic Inflow Boundary

The boundary conditions for the purely subsonic isentropic flow solution at the subsonic inflow boundary two properties are held fixed and one is allowed to float. We hold ρ' and T' fixed at the inflow boundary, both equal to 1.0, and allow V' to float. The application of boundary conditions at the subsonic inflow boundary is exactly the same as in the subsonic-supersonic case.

Supersonic Outflow Boundary

The boundary conditions for the purely subsonic isentropic flow solution at the subsonic inflow boundary two properties are held fixed and one is allowed to float. Since exit pressure is a deciding parameter in the purely subsonic case, we try to fix the dimensionless pressure P'.

$$P' = specified$$

We know from the state equation,

$$P' = \rho' T'$$

We extrapolate the T' and find the value of ρ' using the above relation. This is done to hold the exit pressure at the specified value.

$$T'_N = 2T'_N - 1 - T'_N - 2$$
$$\rho'_N = \frac{P'_N}{T'_N}$$

We extrapolate the V' as

$$V'_N = 2V'_N - 1 - V'_N - 2$$

Now, if we talk about the conservative variables $U1$, $U2$ and $U3$. Since $U1$ and $U2$ are a function of V and ρ, so we linearly extrapolate them as

$$U1_{i=N} = 2U1_{i=N-1} - U1_{i=N-2} \tag{44}$$
$$U2_{i=N} = 2U2_{i=N-1} - U2_{i=N-2} \tag{45}$$

We find $U3_{i=N}$ using the extrapolated V'_N value using the below given relation,

$$U3_{i=N} = \frac{A'_N P'_N}{\gamma - 1} + \frac{\gamma}{2} U2_{i=N} V'_N \tag{46}$$

The values of F_1, F_2, and F_3 at grid point $i = N$ are obtained from the values of U_1, U_2, and U_3 at point $i = N$

5.2. Initial Conditions

The initial conditions for $U1$, $U2$, and $U3$ were synthesized by assuming the following variations of ρ' and T':

$$\rho' = 1.0 \tag{47}$$
$$T' = 1.0 \tag{48}$$

for $0 \leq x' \leq 0.5$

$$\rho' = 1.0 - 0.363(x' - 0.5) \tag{49}$$
$$T' = 1.0 - 0.167(x' - 0.5) \tag{50}$$

for $0.5 \leq x' \leq 1.5$

$$\rho' = 0.637 + 0.363(x' - 1.5) \tag{51}$$
$$T' = 0.835 + 0.165(x' - 1.5) \tag{52}$$

for $1.5 \leq x' \leq 2.5$

$$\rho' = 1.0 \tag{53}$$
$$T' = 1.0 \tag{54}$$

for $0 \leq x' \leq 0.5$

We can compare the above initial conditions of dimensionless ρ' and T' with the Analytical solution.

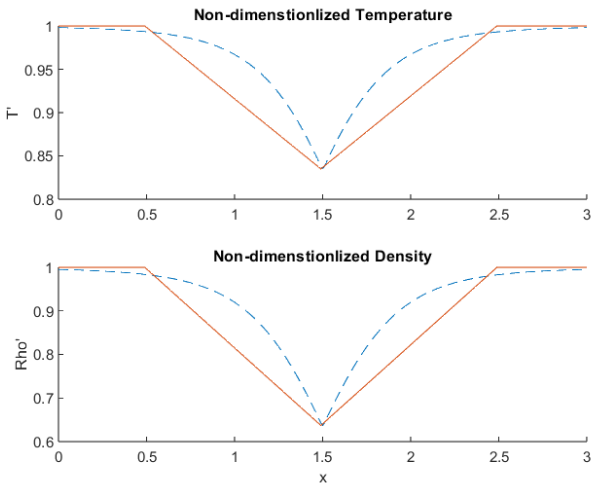

Figure 4. Comparison of Initial Conditions with Analytical Solution

5.3. Calculation of Time Step

The methodology of time step calculation is exactly the same as that of subsonic-subsonic flow simulations. Here, since there are high chances of simulation values blowing up, it becomes imperative to break the simulation wherever we encounter a negative T' during Δt calculation. This is done to avoid imaginary values in our simulation process.

6. MacCormack's Scheme

MacCormack's method is a second-order accurate finite difference method commonly used for solving hyperbolic partial differential equations, such as the Euler equations governing compressible fluid flow. It is a two-step predictor-corrector method that provides a stable and accurate solution for a wide range of flow problems.

The Basic Algorithm

1. Predictor Step: - Calculate the flux derivatives using forward difference:

$$\left(\frac{\partial F}{\partial x}\right)_i^p = \frac{F_{i+1}^n - F_i^n}{\Delta x}, \tag{55}$$

$$\left(\frac{\partial U}{\partial t}\right)_i^p = -\left(\frac{\partial F}{\partial x}\right)_i^p. \tag{56}$$

Finding the predicted values as:

$$U_i^{(n+1)*} = U_i^n + \Delta t \left(\frac{\partial U}{\partial t}\right)_i^p. \tag{57}$$

2. Corrector Step:
Calculate the flux derivatives using backward difference:

$$\left(\frac{\partial F}{\partial x}\right)_i^c = \frac{F_i^{(n+1)*} - F_{i-1}^{(n+1)*}}{\Delta x}, \tag{58}$$

$$\left(\frac{\partial U}{\partial t}\right)_i^c = -\left(\frac{\partial F}{\partial x}\right)_i^c. \tag{59}$$

Finding the corrected values as:

$$U_i^{(n+1)c} = U_i^p + \Delta t \left(\frac{\partial U}{\partial t}\right)_i^c. \tag{60}$$

3. Updation Step:
Finally, we update the solution variables using the average time derivatives:

$$\left(\frac{\partial U}{\partial t}\right)_i^{n+1} = 0.5 * [\left(\frac{\partial U}{\partial t}\right)_i^p + \left(\frac{\partial U}{\partial t}\right)_i^c]. \tag{61}$$

$$U_i^{(n+1)} = U_i + \Delta t \left(\frac{\partial U}{\partial t}\right)_i^{n+1}. \tag{62}$$

6.1. Application to Euler Equations

We will now use the MacCormack scheme on each governing equation individually.

Mass and energy conservation equations:

The conservative forms of generic Euler equations for mass and energy conservation can be written as:

$$\frac{\partial U_1}{\partial t'} = -\frac{\partial F_1}{\partial x'}$$

$$\frac{\partial U_3}{\partial t'} = -\frac{\partial F_3}{\partial x'}$$

Due to their similar mathematical forms, we can apply a similar kind of Maccormack scheme for the above equations which is stated below:

1. Predictor Step: - Calculate the flux derivatives using forward difference:

$$\left(\frac{\partial F}{\partial x}\right)_i^p = \frac{F_{i+1}^n - F_i^n}{\Delta x}, \tag{63}$$

$$\left(\frac{\partial U}{\partial t}\right)_i^p = -\left(\frac{\partial F}{\partial x}\right)_i^p. \tag{64}$$

Finding the predicted values as:

$$U_i^{(n+1)*} = U_i^n + \Delta t \left(\frac{\partial U}{\partial t}\right)_i^p. \tag{65}$$

2. Corrector Step:
Calculate the flux derivatives using backward difference:

$$\left(\frac{\partial F}{\partial x}\right)_i^c = \frac{F_i^{(n+1)*} - F_{i-1}^{(n+1)*}}{\Delta x}, \tag{66}$$

$$\left(\frac{\partial U}{\partial t}\right)_i^c = -\left(\frac{\partial F}{\partial x}\right)_i^c. \tag{67}$$

Finding the corrected values as:

$$U_i^{(n+1)c} = U_i^p + \Delta t \left(\frac{\partial U}{\partial t}\right)_i^c. \tag{68}$$

3. Updation Step:
Finally, we update the solution variables using the average time derivatives:

$$\left(\frac{\partial U}{\partial t}\right)_i^{n+1} = 0.5 * [\left(\frac{\partial U}{\partial t}\right)_i^p + \left(\frac{\partial U}{\partial t}\right)_i^c]. \tag{69}$$

$$U_i^{(n+1)} = U_i + \Delta t \left(\frac{\partial U}{\partial t}\right)_i^{n+1}. \tag{70}$$

Momentum conservation equation:

The conservative forms of generic Euler equations for momentum conservation can be written as:

$$\frac{\partial U2}{\partial t'} = -\frac{\partial F2}{\partial x'} + J2$$

Now, we will state the MacCormack scheme deployed for the above equation in detail.

1. Predictor Step: - Calculate the flux derivatives using forward difference:

$$\left(\frac{\partial F2}{\partial x}\right)_i^p = \frac{F2_{i+1}^n - F_i^n}{\Delta x}, \tag{71}$$

$$\left(\frac{\partial U2}{\partial t}\right)_i^p = -\left(\frac{\partial F2}{\partial x}\right)_i^p + J2_i^n \tag{72}$$

where

$$J2_i^n = \rho_i^n T_i^n \left(\frac{A_{i+1}^n - A_i^n}{dx}\right)$$

Finding the predicted values as:

$$U2_i^{(n+1)*} = U2_i^n + \Delta t \left(\frac{\partial U}{\partial t}\right)_i^p. \tag{73}$$

2. Corrector Step:
Calculate the flux derivatives using backward difference:

$$\left(\frac{\partial F2}{\partial x}\right)_i^c = \frac{F2_i^{(n+1)*} - F2_{i-1}^{(n+1)*}}{\Delta x}, \tag{74}$$

$$\left(\frac{\partial U2}{\partial t}\right)_i^c = -\left(\frac{\partial F2}{\partial x}\right)_i^c + J2_i^* \tag{75}$$

where

$$J2_i^* = \rho_i^* T_i^* \left(\frac{A_{i+1}^* - A_i^*}{dx} \right)$$

Finding the corrected values as:

$$U2_i^{(n+1)c} = U2_i^p + \Delta t \left(\frac{\partial U2}{\partial t} \right)_i^c. \tag{76}$$

3. Updation Step:
Finally, we update the solution variables using the average time derivatives:

$$\left(\frac{\partial U2}{\partial t} \right)_i^{n+1} = 0.5 * [\left(\frac{\partial U2}{\partial t} \right)_i^p + \left(\frac{\partial U2}{\partial t} \right)_i^c]. \tag{77}$$

$$U2_i^{(n+1)} = U2_i + \Delta t \left(\frac{\partial U2}{\partial t} \right)_i^{n+1}. \tag{78}$$

7. Results and Discussions

7.1. Subsonic- Supersonic Flow Simulation Results

In this section, we analyze the results of the subsonic-supersonic flow simulation through the converging-diverging (CD) nozzle. Figures 5, 6, 7, and 8 display the non-dimensionalized values of pressure P', density ρ', temperature T', and Mach number M along the length of the nozzle, respectively. These results are compared to the analytical isentropic flow solutions to assess the accuracy of the numerical model.

Comparison with Analytical Results

The plots attached here were calculated at Courant number at $CFL = 0.5$ and $n = 201$ grid points.

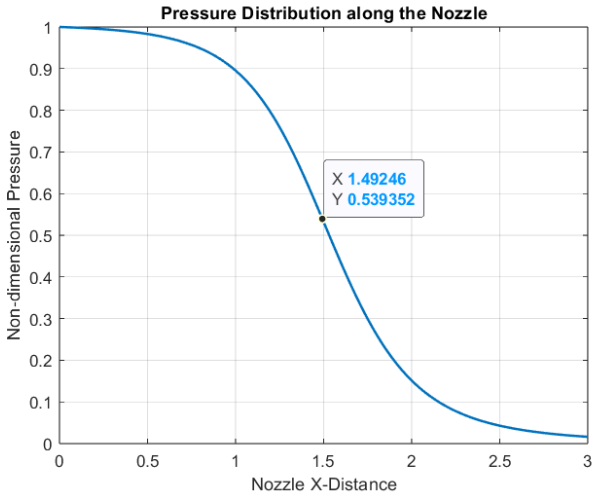

Figure 5. Non-Dimensional Pressure in the nozzle

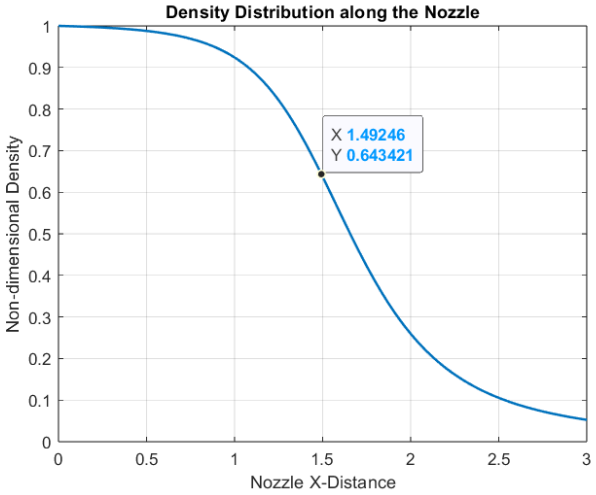

Figure 6. Non-Dimensional Density in the nozzle

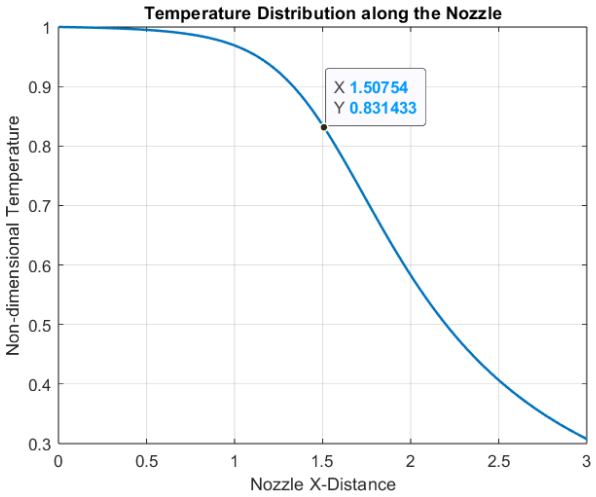

Figure 7. Non-Dimensional Temperature in the nozzle

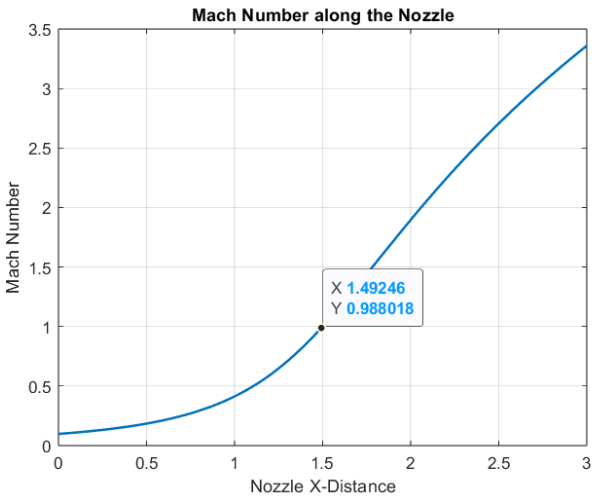

Figure 8. Mach Number in the nozzle

The numerical simulation results closely follow the analytical predictions for an isentropic subsonic-supersonic flow in a CD nozzle. As expected, the flow accelerates in the converging section, reaching

Mach 1 at the throat. Beyond the throat, in the diverging section, the flow smoothly transitions to supersonic speeds. This behavior is accurately captured by the numerical model, as evidenced by the good agreement between the simulation and analytical values for Mach number in Figure 8.

In the pressure plot (Figure5), there is a steady decrease in pressure along the nozzle, consistent with isentropic expansion. Similarly, the density and temperature plots (Figures 6 and 7) show a decreasing trend in the diverging section, following the isentropic flow relations. Minor deviations from the analytical results are observed, particularly near the throat and in the diverging section. These discrepancies are likely due to the numerical diffusion inherent in the finite difference scheme, as well as the limitations imposed by the discretization grid.

Effect of Courant Number on Simulation Stability

The choice of the Courant-Friedrichs-Lewy (CFL) number significantly impacts the stability and accuracy of the simulation. A higher CFL number allows for larger time steps, potentially reducing computational time but increasing the risk of numerical instability. During this simulation, it was observed that CFL numbers approaching 1.0 introduced instability, particularly near the throat where the Mach number rapidly changes. By using a CFL number well below this threshold, the simulation achieved stable results that closely followed the expected trends. For this reason, a CFL number between 0.1 and 0.5 was found to provide a good balance between accuracy and computational efficiency.

Impact of Initial Conditions on Convergence

The choice of initial conditions also plays a crucial role in achieving stable and accurate results. In this study, an initial density profile decreasing linearly along the nozzle length was found to facilitate faster convergence, as it approximates the expected steady-state density distribution. However, using a uniform initial condition resulted in prolonged convergence times and, in some cases, instability, as the system required additional time steps to adjust to the non-uniform flow field. Thus, selecting initial conditions that approximate the steady-state profile can significantly reduce the computational load and enhance stability, as they reduce the number of adjustments required to reach a steady solution.

7.2. Purely Subsonic Flow Simulation Results

This section presents and analyzes the results for the purely subsonic flow simulation through the converging-diverging (CD) nozzle. Figures 9, 10, 11, and 12 show the non-dimensionalized pressure P', density ρ', temperature T', and Mach number M distributions along the nozzle. These simulation results are compared with the analytical isentropic solutions for subsonic flow to evaluate the performance and accuracy of the numerical model.

7.2.1. Comparison with Analytical Results

The plots attached here were calculated at Courant number at $CFL = 0.6$ and $n = 201$ grid points for $max\_iter = 10000$ iterations. The simulation was operated at exit pressure condition $P' = 0.995$.

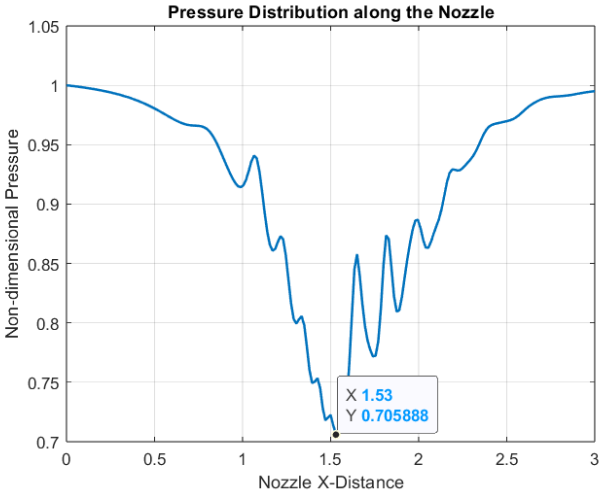

Figure 9. Non-Dimensional Pressure in the nozzle

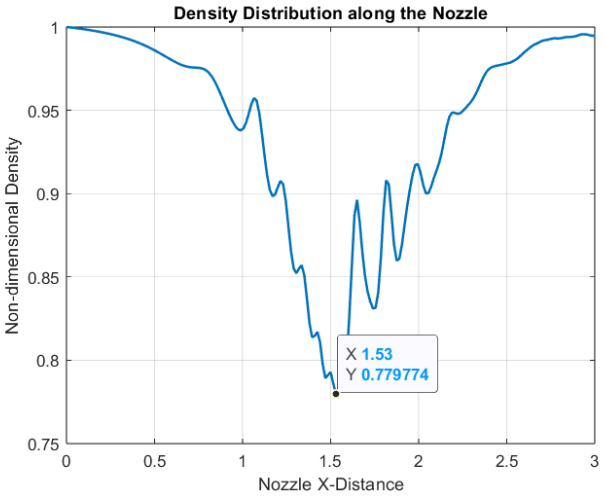

Figure 10. Non-Dimensional Density in the nozzle

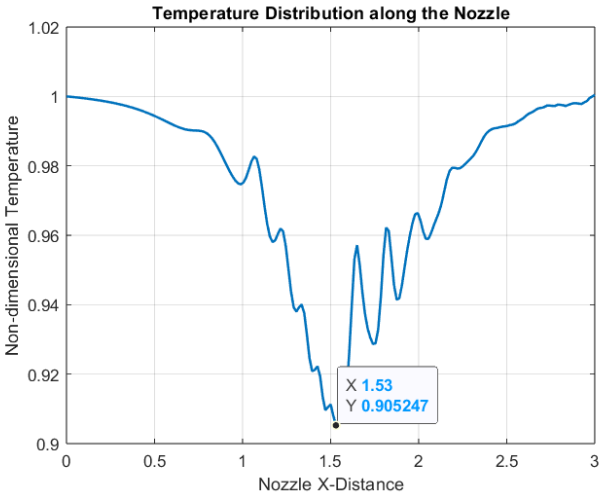

Figure 11. Non-Dimensional Temperature in the nozzle

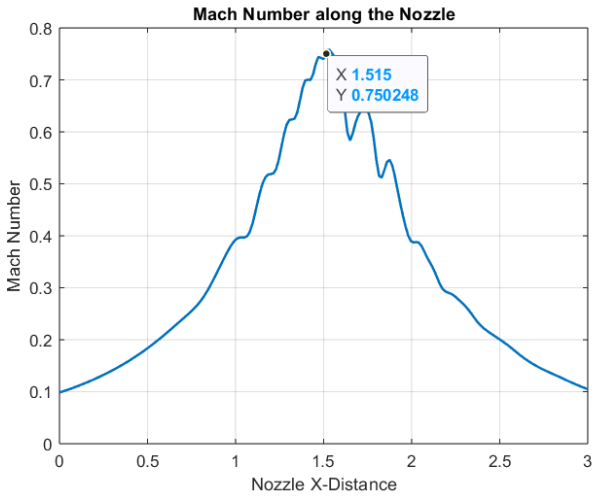

Figure 12. Mach Number in the nozzle

The numerical simulation demonstrates a somewhat in-consistent agreement with the analytical isentropic predictions for purely subsonic flow. Even though the simulation could develop the general trend-line of the flow properties through the nozzle. However, the plots had some major oscillation problems.

The pressure plot in Figure 9 shows a gradual decrease along the converging section and a slight recovery in the diverging section, reflecting the expected behavior in a subsonic nozzle flow. Similarly, the density and temperature profiles (Figures 10 and 11) follow the anticipated trends, with density and temperature decreasing along the nozzle's converging section, then increasing slightly in the diverging section.

The Mach number plot (Figure 12) shows the flow remaining subsonic throughout the nozzle, reaching a maximum value near the throat but remaining below Mach 1, as expected for this flow regime.

7.2.2. Effect of Courant Number on Simulation Stability

In the case of purely Subsonic flows, low CFL number values induced the blowing up of the simulation calculations. Hence, the Courant number was never decreased below 1.4 to avoid oscillatory behavior of the simulation's primitive solution.

7.2.3. Impact of Initial Conditions on Convergence

The initial conditions chosen for the simulation also played a significant role in achieving faster convergence and numerical stability.

8. Acknowledgements

I would like to express my sincere gratitude to Professor Dilip Srinivas Sundaram for providing me with the opportunity to work on this project. I would also like to thank all the Teaching assistants for their invaluable help in sorting out all the bottlenecks throughout this project. Their dedication and expertise were crucial to the success of this project.